# Foamlike Nanostructures Created from Dendritic Platinum Sheets on Liposomes

Yujiang Song,[†] William A. Steen,[†] Donovan Peña,[†] Ying-Bing Jiang,[‡] Craig J. Medforth,[†] Qisheng Huo,[†] Jennifer L. Pincus,[†] Yan Qiu,[†,‡] Darryl Y. Sasaki,[†] James E. Miller,[†] and John A. Shelnutt*[,†,§]

*Surface and Interface Sciences Department, Ceramic Process and Inorganic Materials Department, Chemical Synthesis and Nanomaterials Department, and Corrosion and Electrochemical Sciences Department, Sandia National Laboratories, Albuquerque, New Mexico 87185-1349, Department of Chemical & Nuclear Engineering, The University of New Mexico, Albuquerque, New Mexico 87131, and Department of Chemistry, University of Georgia, Athens, Georgia 30602*

*Received February 15, 2006*

The synthesis of novel dendritic platinum sheets of 2-nm thickness by the reduction of an aqueous metal complex with ascorbic acid in the presence of liposomes is reported. Variation of the reaction conditions, including incorporation of a tin porphyrin photocatalyst within the liposomal bilayer to initiate seed-particle growth, allows access to a diverse range of platinum nanostructures, including dendritic nanosheets of uniform diameters and convoluted foamlike structures composed of interwoven dendritic nanosheets. The mechanism of formation of these nanomaterials is investigated with regard to the photocatalytic generation of platinum nanoparticle seeds, the autocatalytic dendritic growth, and the templating on liposomes. The discrete nanospheres of foamlike platinum are of particular interest, as they may have advantages over conventional platinum black in some applications. For example, they will likely exhibit improved electrical connectivity and mass-transport properties in electrocatalytic applications. Electrochemical CO-stripping measurements and $N_2$ adsorption experiments show that the nanospheres of foamlike platinum possess high surface areas. In addition, these platinum foam nanospheres are as active as commercial platinum black in catalyzing the four-electron oxygen reduction reaction.

## Introduction

Platinum has many technological applications[1−3] such as in sensors,[4−6] biosensors,[7] and other devices,[8−10] as a catalyst for reduction of tailpipe emissions, as an electrocatalyst in polymer electrolyte membrane (PEM) fuel cells,[11,12] and as a catalyst in solar water-splitting devices.[13,14] Because of the limited supply and high cost of Pt, researchers are developing methods for eliminating or reducing the precious metal content of these catalysts. One way to minimize Pt usage is to increase catalytic efficiency by nanostructuring the platinum metal. As catalytic or device efficiency may depend on both the size and the shape of the platinum material,[15−18] the preparation of nanostructured platinum with specific structural features is an area of considerable interest.

Nanostructured platinum has been prepared using a range of techniques. Nanotubes[19] and mesoporous platinum films[20,21] have been obtained by chemical and electrochemical reduction of platinum salts confined within the aqueous environment of the lyotropic liquid crystalline phases of surfactants. The templating channels[22] of porous materials have also been used to produce nanoparticles,[23−25] nanowires,[26−28] or nano-

* To whom correspondence should be addressed. E-mail: jasheln@unm.edu.
† Sandia National Laboratories.
‡ The University of New Mexico.
§ University of Georgia.

(1) Scott, D. S.; Hafele, W. *Int. J. Hydrogen Energy* **1990**, *15*, 727−737.
(2) Kordesch, K. V.; Simader, G. R. *Chem. Rev.* **1995**, *95*, 191−207.
(3) Service, R. F. *Science* **1999**, *285*, 682−685.
(4) Makto, I.; Gaidi, M.; Hazemann, J. L.; Chenevier, B.; Labeau, M. *Sens. Actuators, B* **1999**, *59*, 210−215.
(5) Bittencourt, C.; Llobet, E.; Ivanov, P.; Correig, X.; Vilanova, X.; Brezmes, J.; Hubalek, J.; Malysz, K.; Pireaux, J. J.; Calderer, J. *Sens. Actuators, B* **2004**, *97*, 67−73.
(6) Matsumiya, M.; Shin, W.; Izu, N.; Murayama, N. *Sens. Actuators, B* **2003**, *93*, 309−315.
(7) Hrapovic, S.; Liu, Y. L.; Male, K. B.; Luong, J. H. T. *Anal. Chem.* **2004**, *76*, 1083−1088.
(8) Melosh, N. A.; Boukai, A.; Diana, F.; Cerardot, B.; Badolato, A.; Petroff, P. M.; Heath, J. R. *Science* **2003**, *300*, 112−115.
(9) Roach, P. R.; Takano, Y.; Hilleke, R. O.; Vrtis, M. L.; Jin, D.; Sarma, B. K. *Cryogenics* **1986**, *26*, 319−321.
(10) De, S.; Pal, A.; Pal, T. *Langmuir* **2000**, *16*, 6855−6861.
(11) Rolison, D. R. *Science* **2003**, *299*, 1698−1701.
(12) Antolini, E. *Mater. Chem. Phys.* **2003**, *78*, 563−573.
(13) Cameron, P. J.; Peter, L. M.; Zakeeruddin, S. M.; Gratzel, M. *Coord. Chem. Rev.* **2004**, *248*, 1447−1453.
(14) Fang, X. M.; Ma, T. L.; Guan, G. Q.; Akiyama, M.; Abe, E. *J. Photochem. Photobiol.* **2004**, *164*, 179−182.
(15) Narayanan, R.; El-Sayed, M. A. *J. Phys. Chem. B* **2004**, *108*, 5726−5733.
(16) Narayanan, R.; El-Sayed, M. A. *Nano Lett.* **2004**, *4*, 1343−1348.
(17) Narayanan, R.; El-Sayed, M. A. *J. Am. Chem. Soc.* **2004**, *126*, 7194−7195.
(18) Narayanan, R.; El-Sayed, M. A. *Langmuir* **2005**, *21*, 2027−2033.
(19) Kijima, T.; Yoshimura, T.; Uota, M.; Ikeda, T.; Fujikawa, D.; Mouri, S.; Uoyama, S. *Angew. Chem., Int. Ed.* **2004**, *43*, 228−232.
(20) Attard, G. S.; Bartlett, P. N.; Coleman, N. R. B.; Elliott, J. M.; Owen, J. R.; Wang, J. H. *Science* **1997**, *278*, 838−840.
(21) Attard, G. S.; Goltner, C. G.; Corker, J. M.; Henke, S.; Templer, R. H. *Angew. Chem., Int. Ed. Engl.* **1997**, *36*, 1315−1317.
(22) Possin, G. E. *Rev. Sci. Instrum.* **1970**, *41*, 772−774.
(23) Hulteen, J. C.; Martin, C. R. *J. Mater. Chem.* **1997**, *7*, 1075−1087.
(24) Che, G. L.; Lakshmi, B. B.; Fisher, E. R.; Martin, C. R. *Nature* **1998**, *393*, 346−349.
(25) Joo, S. H.; Choi, S. J.; Oh, I.; Kwak, J.; Liu, Z.; Terasaki, O.; Ryoo, R. *Nature* **2001**, *412*, 169−172.

10.1021/cm060384d CCC: $33.50 
Published on Web 03/22/2006

wire networks[29,30] depending on the reaction conditions. Alternatively, shape-controlled nanocrystals, including tetrahedral, cubic, irregular-prismatic, icosahedral, and cubo-octahedral particles, have been synthesized by interfacially directed growth using capping polymers to control the relative growth rates of different crystalline faces.[31,32] The reduction of platinum chloride intercalation compounds confined between graphitic layers produces platinum nanosheets.[33,34] The polyol method combined with the introduction of a trace amount of $Fe^{2+}$ (or $Fe^{3+}$) has also recently been used to synthesize large quantities of single crystalline nanowires.[35] Polypeptides,[36] peptide nanotubes,[37] and peptide-functionalized[38] peptide nanotubes have also been used to template the growth of nanostructured platinum. Finally, hollow nanospheres[39] have been prepared by the nanoparticle templating method,[40−42] which involves a galvanic replacement reaction between sacrificial nanoelectrodes and a metal complex.

Recently, our group has developed an approach to the rational synthesis of nanostructured platinum based on the reduction of platinum complexes with L-ascorbic acid (AA) in the presence of surfactant templates.[43] Depending on the surfactant assemblies used in the reaction (e.g., liposomes or micelles), it is possible to obtain dendritic metal sheets or spherical nanostructures. Uniform-sized globular nanodendrites of a particular average diameter are obtained by using a tin porphyrin photocatalyst to rapidly produce a large number of platinum seed particles at the beginning of the reaction according to the following equations:

$$\mathrm{SnP} + h\nu \rightarrow \mathrm{SnP}^*$$

$$\mathrm{SnP}^* + \mathrm{ED} \rightarrow \mathrm{SnP}^{\bullet -} + \mathrm{ED}_{ox}$$

$$2\mathrm{SnP}^{\bullet -} + \mathrm{Pt}^{2+} \rightarrow 2\mathrm{SnP} + \mathrm{Pt}^0$$

where the photocatalyst SnP is Sn(IV) octaethylporphyrin (SnOEP) in the present work and AA is used as the electron donor (ED). The Pt seeds then grow into the dendrites by catalytic oxidation of AA and reduction of Pt complex. SnOEP is hydrophobic and thus is expected to reside in the interior of surfactant micelles and, for liposomes, between the surfactant layers. The principle of this photocatalytic seeding strategy is to provide nearly equal growth times for each of the nucleation centers. The photocatalytic seeding strategy can be contrasted to the spontaneous seed formation, which occurs at random intervals and results in different growth periods and a wide range of nanodendrite sizes. The preferred average size is obtained by choosing the ratio between the number of seeds and the total amount of metal complex provided. The number of seeds can be chosen by varying the photocatalyst concentration and the light exposure time. Interestingly, the spherical nanodendrites produced in this manner are functional nanostructures due to the presence of attached tin porphyrin photocatalyst (e.g., they can produce hydrogen from water using visible light and electrons supplied by a sacrificial electron donor).[43]

Our earlier work was mainly focused on the synthesis of nanoscale spherical Pt dendrites using micelles as templates, but we also showed that dendritic Pt sheets of nanoscale thickness could be formed under similar solution conditions when liposomes were used as templates.[43] Herein, we investigate in detail the synthesis of Pt nanostructures using 1,2-dioctadecanoyl-*sn*-glycero-3-phosphocholine (DSPC) liposomes as templates. There are only a few studies in the literature describing the use of liposome templates to grow nanomaterials, such as to template the growth of silica[44−48] and calcium phosphate[49] nanostructures. We now show that liposomes with and without incorporated porphyrin photocatalysts can be used to generate a range of novel platinum nanostructures, ranging from small uniform dendritic sheets to large circular dendritic sheets to various foamlike platinum structures composed of convoluted dendritic sheets. The size and other features of these dendritic nanostructures are fine-tuned by using the photocatalytic properties of the tin porphyrin residing in the liposomal bilayer to control the initial number of platinum growth sites and/or by differing the experimental conditions such as using liposomes made in water or in AA solution to influence the extent of liposomal aggregation. The time evolution of these structures was examined to help to elucidate the growth mechanism of these novel platinum metal structures.

Studies of the synthesis of the foamlike nanospheres show that they can be prepared on a large scale. $N_2$ adsorption and CO-stripping measurements show that the foam balls have high surface areas comparable to some commercial

(26) Han, Y. J.; Kim, J. M.; Stucky, G. D. *Chem. Mater.* **2000**, *12*, 2068−2069.
(27) Liu, Z.; Sakamoto, Y.; Ohsuna, T.; Hiraga, K.; Terasaki, O.; Ko, C. H.; Shin, H. J.; Ryoo, R. *Angew. Chem., Int. Ed.* **2000**, *39*, 3107−3110.
(28) Sakamoto, Y.; Fukuoka, A.; Higuchi, T.; Shimomura, N.; Inagaki, S.; Ichikawa, M. *J. Phys. Chem. B* **2004**, *108*, 853−858.
(29) Shin, H. J.; Ko, C. H.; Ryoo, R. *J. Mater. Chem.* **2001**, *11*, 260−261.
(30) Shin, H. J.; Ryoo, R.; Liu, Z.; Terasaki, O. *J. Am. Chem. Soc.* **2001**, *123*, 1246−1247.
(31) Ahmadi, T. S.; Wang, Z. L.; Green, T. C.; Henglein, A.; El-Sayed, M. A. *Science* **1996**, *272*, 1924−1926.
(32) Ahmadi, T. S.; Wang, Z. L.; Henglein, A.; El-Sayed, M. A. *Chem. Mater.* **1996**, *8*, 1161−1163.
(33) Shirai, M.; Igeta, K.; Arai, M. *Chem. Commun.* **2000**, 623−624.
(34) Shirai, M.; Igeta, K.; Arai, M. *J. Phys. Chem. B* **2001**, *105*, 7211−7215.
(35) Chen, J. Y.; Herricks, T.; Geissler, M.; Xia, Y. N. *J. Am. Chem. Soc.* **2004**, *126*, 10854−10855.
(36) Naik, R. R.; Jones, S. E.; Murray, C. J.; McAuliffe, J. C.; Vaia, R. A.; Stone, M. O. *Adv. Funct. Mater.* **2004**, *14*, 25−30.
(37) Song, Y. J.; Challa, S. R.; Medforth, C. J.; Qiu, Y.; Watt, R. K.; Pena, D.; Miller, J. E.; Van Swol, F.; Shelnutt, J. A. *Chem. Commun.* **2004**, 1044−1045.
(38) Yu, L. T.; Banerjee, I. A.; Matsui, H. *J. Mater. Chem.* **2004**, *14*, 739−743.
(39) Liang, H. P.; Zhang, H. M.; Hu, J. S.; Guo, Y. G.; Wan, L. J.; Bai, C. L. *Angew. Chem., Int. Ed.* **2004**, *43*, 1540−1543.
(40) Sun, Y. G.; Xia, Y. N. *Science* **2002**, *298*, 2176−2179.
(41) Sun, Y. G.; Mayers, B. T.; Xia, Y. N. *Nano Lett.* **2002**, *2*, 481−485.
(42) Sun, Y. G.; Mayers, B.; Xia, Y. N. *Adv. Mater.* **2003**, *15*, 641−646.
(43) Song, Y. J.; Yang, Y.; Medforth, C. J.; Pereira, E.; Singh, A. K.; Xu, H. F.; Jiang, Y. B.; Brinker, C. J.; van Swol, F.; Shelnutt, J. A. *J. Am. Chem. Soc.* **2004**, *126*, 635−645.
(44) Dubois, M.; Gulikkrzywicki, T.; Cabane, B. *Langmuir* **1993**, *9*, 673−680.
(45) Tanev, P. T.; Pinnavaia, T. J. *Science* **1996**, *271*, 1267−1269.
(46) Tanev, P. T.; Pinnavaia, T. J. *Supramol. Sci.* **1998**, *5*, 399−404.
(47) Hubert, D. H. W.; Jung, M.; German, A. L. *Adv. Mater.* **2000**, *12*, 1291−1294.
(48) Hubert, D. H. W.; Jung, M.; Frederik, P. M.; Bomans, P. H. H.; Meuldijk, J.; German, A. L. *Adv. Mater.* **2000**, *12*, 1286−1290.
(49) Schmidt, H. T.; Ostafin, A. E. *Adv. Mater.* **2002**, *14*, 532−535.

platinum black materials. These foam balls are also found to be as good as a fuel-cell grade platinum black for catalyzing the oxygen reduction reaction (ORR). In addition, they are highly porous, self-supporting nanostructures that possess a high degree of electrical connectivity because of their dendritic morphology. These features potentially offer increased performance in catalytic and electrocatalytic applications (e.g., in PEM fuel cells and photoelectrochemical solar cells). In the biological arena, the tin porphyrin photocatalytic seeding method might be used to grow platinum nanoparticles (or small dendrites) near the sites of porphyrin molecules or porphyrin-labeled biological molecules in membranes to serve as "nanotags" that reveal the location of the porphyrin labels when imaged by transmission electron microscopy (TEM).

## Materials and Methods

**Materials.** Potassium tetrachloroplatinate ($K_2PtCl_4$; 99.99%), AA (99+%), DSPC (99%), and cholesterol (99+%) were of the highest purity available and were used as received from Sigma-Aldrich (St. Louis, MO). Tin(IV) octaethylporphyrin dichloride was obtained from Porphyrin Products (Logan, UT) and used without further purification. All aqueous solutions were prepared with ultrapure water from a Barnstead Nanopure water system (Chesterland, OH).

A stock solution of the platinum(II) complex (20 mM) was prepared by dissolving $K_2PtCl_4$ in water and allowing it to age for at least 24 h before use. Aging results in disproportionation of the complex into an equilibrium mixture of 42% $Pt(H_2O)_2Cl_2$, 53% $Pt(H_2O)Cl_3^-$, and 5% $PtCl_4^{2-}$.[50] An AA stock solution (150 mM) was freshly prepared before each reaction because it gradually oxidizes in air. The SnOEP stock solution (1 mM) was prepared by dissolving Sn(IV) octaethylporphyrin dichloride in chloroform. Stock solutions of DSPC (1.0 mM) and cholesterol (1.0 mM) were prepared by dissolving the respective compounds in chloroform.

Multilamellar liposomes (vesicles) were prepared by adding DSPC (7.9 mg) to 10 mL of AA solution (150 mM) followed by mild sonication for 2 min using a Fisher Scientific ultrasonic cleaner FS14H (Pittsburgh, PA), giving a final DSPC concentration of 1 mM. The average diameter of the vesicles (400 nm) was determined by dynamic light scattering using a Beckman Coulter N5 submicrometer particle size analyzer as described previously.[43]

To prepare the unilamellar liposomes, 5 mL of the 1.0 mM DSPC and the 1.0 mM cholesterol stock solutions were mixed in a glass tube; lipid films formed on the glass wall after evaporating the chloroform under vacuum. After drying overnight, 10 mL of AA solution (150 mM) was added, and the mixture was heated for 1 h at 65 °C in a water bath. The sample was then vortexed to facilitate the formation of multilamellar vesicles, and the mixture was subjected to 10 freeze−thaw cycles. Finally, the mixture was extruded through an 80-nm, 100-nm, or 200-nm porous polycarbonate filter, and the extrusion process was repeated a total of 10 times. The average diameter of the unilamellar liposomes measured by dynamic light scattering was approximately 60−80 nm when the 80-nm filter was used and approximately 110−120 nm and 140−170 nm when 100-nm and 200-nm filters, respectively, were used. Unilamellar liposomes were also prepared by adding water instead of the AA solution to the dried lipids.

Liposome suspensions, made either with an AA solution or with water, were also prepared by the addition of varying amounts of SnOEP stock solution to the lipids prior to drying, giving a SnOEP concentration in the final reaction mixture of 1.6−23.3 $\mu$M depending upon the experiment.

**Synthesis of Dendritic Nanosheets and Foamlike Nanostructures without Photocatalytic Control.** Circular dendritic platinum nanosheets with diameters of 30−500 nm were prepared using the multilamellar DSPC vesicles in AA solution (150 mM) as templates. The average diameter of the multilamellar DSPC liposomal templates used in the reaction was 400 nm. To prepare the dendritic nanosheets, 1 mL of a suspension of multilamellar DSPC liposomes (1 mM DSPC) in AA (150 mM) was mixed with 1 mL of the aged platinum complex (20 mM) in a glass reaction vessel. The reaction mixture was left under ambient conditions for at least 100 min to ensure that Pt reduction was complete before the samples were taken for imaging studies.

The platinum foam nanospheres were synthesized by adding 1 mL of the suspension of the unilamellar liposomes prepared in water to a glass reaction vessel, followed by the addition of 1 mL of aged platinum complex (20 mM) and 26.4 mg of solid AA. Immediately after mixing, the cloudy liposome suspension appears to flocculate. The reaction mixture was swirled to dissolve the AA and left under ambient conditions for at least 100 min before samples were taken for imaging studies. The final concentrations of the platinum complex (10 mM) and AA (75 mM) were the same as those used to prepare the circular dendritic Pt nanosheets. The foamlike nanospheres were synthesized using liposomes with average diameters in the ranges of 60−80, 110−120, and 140−170 nm.

The synthesis of the foam nanospheres was also carried out on a large scale (initial Pt content: 390 mg) to generate sufficient quantities of material to allow surface area measurements and studies of their catalytic properties. The experimental procedure used was the same as that used in the small-scale reaction except that the quantities of reagents were increased by a factor of 100 (100 mL of unilamellar liposomes, 100 mL of aged platinum complexes, 2.64 g of AA). The large-scale syntheses were carried out using the liposomes prepared with 80-nm or 200-nm filters (average diameters 78 or 140 nm). The foam nanospheres were purified by batch processing of 50-mL quantities of the reaction mixture. The batches were initially centrifuged at 3500 rpm for at least 5 min using an IEC Centra MP4R Centrifuge (Golden, CO). The supernatant was then removed, fresh Nanopure water was added to the black precipitate, and the material was re-suspended by mild sonication for 30 min. The centrifuging/re-suspension procedure was repeated five more times to remove as much surfactant, salts, and other impurities as possible. The resulting black slurry was then dried in an oven for 12 h at 75 °C prior to being used in the surface-area and catalysis studies. Thermal analysis (see below) indicated that the material was greater than 98% platinum by weight. The yield of platinum foam spheres was 299 mg (75% based on the starting platinum content of the complex and assuming 98% purity of the nanospheres).

**Synthesis of Circular Groups of Nanoparticles and Small Uniform-Sized Dendritic Sheets Associated with Individual Liposomes Using Photocatalytic Control.** The use of SnOEP in the reaction to rapidly generate platinum growth centers for the dendrites was investigated for the unilamellar liposomes prepared in water or in AA solution (150 mM). For these nanotagging experiments, liposomes were prepared in AA solutions and in water with 23.3 $\mu$M and 1.6 $\mu$M SnOEP, respectively. In a typical synthesis using liposomes prepared in AA, the suspension of the liposomes (1 mL) was mixed with 1 mL of aged platinum complex (4 mM) and irradiated for 30 min with incandescent light (800 $nmol \cdot cm^{-2} \cdot s^{-1}$) before the samples were taken for imaging studies.

(50) Ciacchi, L. C.; Pompe, W.; De Vita, A. *J. Am. Chem. Soc.* **2001**, *123*, 7371−7380.

For the case of liposomes prepared in water, AA powder was added after adding the Pt complex. The light intensity was measured with a Hansatech instrument (Norfolk, U.K.).

**Synthesis of Foamlike Platinum Nanostructures with Photocatalytic Control.** A variety of platinum foam nanostructures (shown in Figure 7) were synthesized by adding 1 mL of the suspension of the unilamellar liposomes containing SnOEP (2.7 $\mu$M) prepared in water to a glass reaction vessel, followed by the addition of 1 mL of aged platinum complex (20 mM) and solid AA (26.4 mg). The reaction mixture was swirled to dissolve the AA, and the solution was irradiated with incandescent light (800 nmol·cm$^{-2}$·s$^{-1}$) for 0, 3, 5, and 10 min, respectively. Immediately after mixing, the cloudy liposome suspension appears to flocculate. The reaction mixture was left in the dark until a total time of 100 min had elapsed, and samples were then taken for imaging studies.

**Electron Microscopy and X-ray Diffraction Studies.** TEM (200 keV, JEOL 2010), high-resolution TEM, high-angle annular dark-field (HAADF) scanning TEM (200 keV, JEOL 2010F), and scanning electron microscopy (SEM, 1−30 keV, S-5200) were performed on the Pt nanostructures. The samples for TEM analysis were prepared by adding drops of the colloidal suspensions onto a standard holey-carbon-coated copper grid and wicking away the excess liquid with a tissue paper. The grids were then washed several times with Nanopure water to remove any remaining metal salts and surfactant molecules and air-dried for at least 2 h before imaging. The samples for SEM characterization were prepared using the same procedure with doped silicon wafers instead of holey-carbon copper grids. X-ray diffraction (XRD) spectra were recorded on a Siemens D500 diffractometer using Ni-filtered Cu K$\alpha$ radiation with $\lambda = 1.5418$ Å in $\theta-2\theta$ scan mode using a step size of 0.05° and a 30-s step time. The sample was supported on a sheet of amorphous plastic.

**Thermal Analysis and Surface Area Measurements.** The composition of the Pt foam nanospheres obtained from the large-scale synthesis was investigated using differential thermal analysis and thermogravometric analysis (DTA/TGA). The experiments were performed using a STD 2960 Simultaneous DTA/TGA-DSC 2010 instrument with air as the processing atmosphere and a heating rate of 10 °C/min.

The surface areas of the platinum foam spheres from large-scale syntheses with 78-nm and 140-nm liposomes were determined by $N_2$ adsorption experiments. The samples were degassed at 100 °C and 0.01 Torr for at least 12 h before measurement. The surface area measurements were conducted using an Autosorb-6 Quantachrome instrument (Boynton Beach, FL). The surface areas were calculated from the Brunauer−Emmet−Teller (BET) equation using a nitrogen molecular area of 0.162 nm$^2$. The linear region between 0.05 and 0.3 relative pressures gives a least-squares coefficient $R^2 > 0.999$ for at least seven adsorption points. Fuel cell grade platinum black powders from ETEK and Sigma-Aldrich having a surface area of 30 m$^2$/g were used for comparison with our platinum nanomaterials.

**Electrochemical Experiments.** Electrochemical experiments were performed using the thin film voltammetric techniques developed by Schmidt et al.[51] Electrodes were prepared by first making aqueous slurries of the nanostructured Pt powders as well as a standard Pt black (ETEK C-6 100% Pt black Fuel Cell Grade) with Pt concentrations from 0.2 to 1.2 g/L. Multiple slurries were prepared to estimate uncertainties in the sample preparation procedures and the experimental measurements. Glassy carbon electrodes (GCE) 3 mm in diameter (area = 0.0707 cm$^2$) were polished with 0.05 $\mu$m Bio-Analytical Systems (BAS) alumina paste and sonicated in methanol prior to deposition of the catalyst powders. The aqueous slurries were sonicated for a minimum of 15 min; 5 $\mu$L of the sonicated slurry was then deposited onto the cleaned GCE. The catalyst was allowed to dry before a thin-layer coating (~0.5 $\mu$m) of Nafion was applied (Aldrich Nafion 1100, 5 wt % in methanol further diluted 1:10 in methanol). The resulting catalyst loadings were between 1 and 6 $\mu$g of Pt or between 14 and 85 $\mu$g of Pt/cm$^2$.

A standard three electrode cell was employed with a saturated calomel electrode as the reference electrode, a Pt wire as the counter electrode, and the platinum catalyst-coated GCE as the working electrode (WE). All potentials are referenced to a reversible hydrogen electrode (RHE). A BAS 100B potentiostat and a 628−10 Metrohm rotating disk assembly were used for the CO-stripping and ORR experiments. Both CO-stripping and ORR experiments were performed at the laboratory temperature (20−22 °C). Prior to all voltammetric experiments, each catalyst was electrochemically conditioned in a 0.5 M $H_2SO_4$ solution (Fisher Scientific, 36 N reagent A.C.S. grade $H_2SO_4$ diluted with deionized water) by briefly (5−10 s) polarizing the WE to potentials where hydrogen evolution occurs (i.e., less than 0 $mV_{RHE}$).

In the CO-stripping measurements, the evolved $H_2$ was removed from the WE by rotating the electrode, and then CO was adsorbed onto the electrocatalyst surface by holding the potential at 100 $mV_{RHE}$ for 3 min in a 0.5 M $H_2SO_4$ solution saturated with ultrahigh purity (UHP) CO. This was done while rotating the WE at 1000 rpm to increase mass transfer. (Preliminary experiments with longer CO deposition times did not result in more CO being deposited, so the conclusion was drawn that 3 min at 1000 rpm saturates the Pt.) The potential was then swept at 20 mV/s from 100 to 1265 $mV_{RHE}$. Between 4 and 12 separate electrodes for each catalyst were tested at least two times each, resulting in between 8 and 32 separate measurements to determine average values and standard deviations. Representative CO-stripping voltammograms are shown in Figure S9 (Supporting Information), and the procedures used in the calculation of the electroactive surface areas are described in Supporting Information (see Supporting Information text and Figure S10).

For the ORR experiments, the electrocatalyst surface was first electrochemically conditioned and the evolved $H_2$ was removed as described above. The potential was then swept from 1265 to 165 $mV_{RHE}$ at 5 mV/s while the WE was rotated at 500, 1000, 1500, 2000, and 2500 rpm in a UHP $O_2$ saturated 0.5 M $H_2SO_4$ solution. For the experiments, four different electrodes with various loadings were tested for each electrocatalyst material. The Levich and Tafel slope analysis of the ORR data is described in the Supporting Information text and in Figures S11−S13.

## Results and Discussion

**Synthesis of Platinum Nanoparticles and Dendritic Platinum Nanosheets.** In a previous paper, we showed that it is possible to prepare several kinds of dendritic platinum nanostructures using surfactants as templates.[43] In the presence of sodium dodecyl sulfate or Brij-35 micelles, spherical platinum nanodendrites could be obtained from the AA reduction of the Pt complex, and the size and size distribution of these nanodendrites could be controlled by varying the platinum concentration and/or by using a tin porphyrin photocatalyst to generate a large initial population of platinum seed particles that then grow autocatalytically. Unilamellar DSPC/cholesterol liposomes or multilamellar DSPC liposomes were also briefly examined as templates.

(51) Schmidt, T. J.; Gasteiger, H. A.; Stab, G. D.; Urban, P. M.; Kolb, D. M.; Behm, R. J. *J. Electrochem. Soc.* **1998**, *145*, 2354−2358.

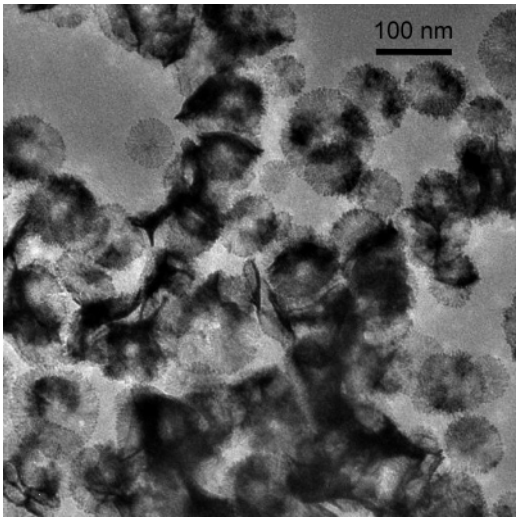


**Figure 1.** TEM images of the mixture of dendritic platinum nanostructures grown on 170-nm liposomes prepared in 150 mM AA. Reaction conditions: [Pt] = 10 mM; [AA] = 75 mM; [DSPC] = 0.25 mM; [cholesterol] = 0.25 mM.

Depending upon the conditions used in the reaction, the liposomal templates resulted in the formation of circular nanosheets as well as foamlike structures composed of convoluted dendritic Pt nanosheets. In this section, we present a comprehensive study of the use of liposomal templating and the photocatalytic seeding strategy to produce a variety of novel dendritic platinum nanostructures. These methods have now been refined, making possible the synthesis of pure forms of the flat dendritic nanosheets and various foam nanostructures (nanospheres and monoliths). The experiments also confirm our earlier assertion[43] that, whether the seeds are produced by rapid photocatalytic reduction of the complex or by slow spontaneous reduction of the complex, the seeds obtained rapidly grow into dendrites by autocatalytic reduction of the Pt complex at the metal surface. As will be seen, the data are best explained by this dendritic growth mechanism rather than a mechanism based on initial formation of many Pt nanoparticles followed by their aggregation to form the dendrites (as has been suggested in two recent related studies).[52,53]

When unilamellar liposomes prepared in an aqueous AA solution (150 mM, pH 3) are used in the reaction ([Pt] = 10 mM; [AA] = 75 mM; [DSPC] = 0.25 mM; [cholesterol] = 0.25 mM), the product obtained consists of a mixture of circular nanosheets of varying sizes plus the disordered aggregated forms of these sheets (Figure 1). Changing the Pt concentration and/or adding a tin porphyrin photocatalyst to the liposomes and irradiating with visible light dramatically alters the structure of the platinum material obtained from the reaction. For example, Figure 2a shows a representative TEM image obtained when a high concentration of the porphyrin photocatalyst (23.3 $\mu$M SnOEP) in the liposomes and a low concentration of platinum complex (2 mM) are used. These reaction conditions produce circular areas that contain a large number of 3-nm platinum particles. These circular areas of particles are approximately the same size as the 65-nm unilamellar liposomes used in the reaction. In other words, the platinum particles from each circular area likely originate from a single collapsed liposome, which cannot itself be seen because of the inherently low contrast of the hydrocarbon-based liposomal structures in TEM. In this regard, the nanoparticles may serve as "nanotags" that reveal the locations of the SnOEP molecules in the liposomal bilayer. We are currently investigating applications of this photocatalytic nanotagging technique using a range of metals, lipid membranes, and other biologically relevant systems. Using the same reaction conditions that produced the nanotagged liposomes in Figure 2a, except for a higher platinum concentration (10 mM versus 2 mM of Pt complex), yields the expected increase in platinum dendrite size and liposomal coverage and also increased aggregation of the Pt nanostructures (Figure 2b).

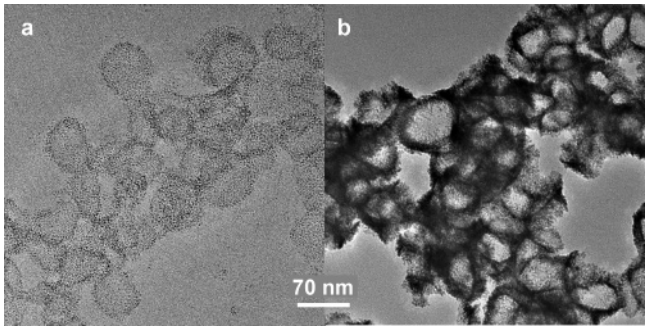


**Figure 2.** (a) TEM images of platinum nanoparticles grown on 65-nm liposomes prepared in 150 mM AA at (a) low (2 mM) and (b) high (10 mM) concentrations of platinum. Other reaction conditions: [AA] = 75 mM; [DSPC] = 0.25 mM; [cholesterol] = 0.25 mM; [SnOEP] = 23.3 $\mu$M.

The size of the nanotags can be altered by adjusting the amount of Pt metal available per seed particle produced by a porphyrin photocatalyst molecule. With liposomes containing a lower SnOEP concentration (1.6 $\mu$M vs 23.3 $\mu$M) and prepared in water, similar solution and illumination conditions decrease the number of seeds to produce small dendrites approximately 10 nm in diameter (Figure 3) instead of the 3-nm nanoparticles seen in Figure 2a. In fact, the small dendrites often form circular groups with the approximate diameter (140 nm) of the liposomes used in the reaction (see inset of Figure 3), indicating that the liposomes collapse as a unit onto the TEM grid. The distribution of the dendrites in the circles reveals an even coverage, suggesting that the porphyrin photocatalyst that initiates their growth is also evenly distributed over the liposomal bilayer. Increasing the platinum concentration from 2 mM to 10 mM again results in the formation of aggregated structures (similar to those in Figure 2b). The aggregation of these platinized structures may result from liposomal aggregation induced by the higher ionic strength of the reaction medium with 10 mM Pt complex (see discussion below).

It is difficult to obtain pure forms of large flat dendritic nanosheets using the unilamellar liposomes as templates mainly because of the limited size of the liposomes and the required high concentration of Pt complex (which causes liposomal aggregation). Larger templating surfactant structures are provided by the *multilamellar* liposomes or vesicles

(52) Ewers, T. D.; Sra, A. K.; Norris, B. C.; Cable, R. E.; Cheng, C. H.; Shantz, D. F.; Schaak, R. E. *Chem. Mater.* **2005**, *17*, 514−520.
(53) Ramirez, E.; Jansat, S.; Philippot, K.; Lecante, P.; Gomez, M.; Masdeu-Bulto, A. M.; Chaudret, B. *J. Organomet. Chem.* **2004**, *689*, 4601−4610.

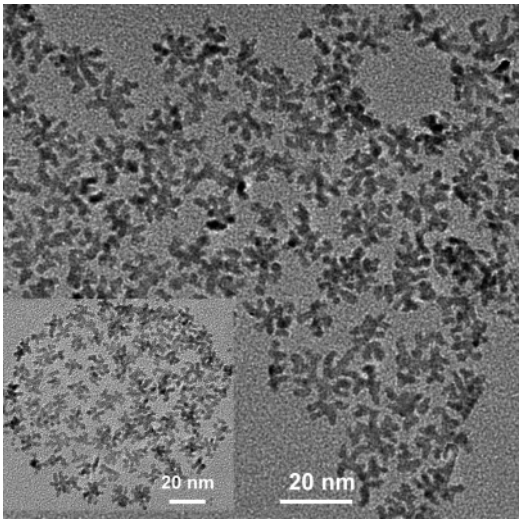


**Figure 3.** TEM images of platinum nanoparticles grown on 140 nm liposomes prepared in water with a low concentration of Pt complex (2 mM). Reaction conditions: [AA] = 75 mM; [DSPC] = 0.25 mM; [cholesterol] = 0.25 mM; [SnOEP] = 1.6 $\mu$M.

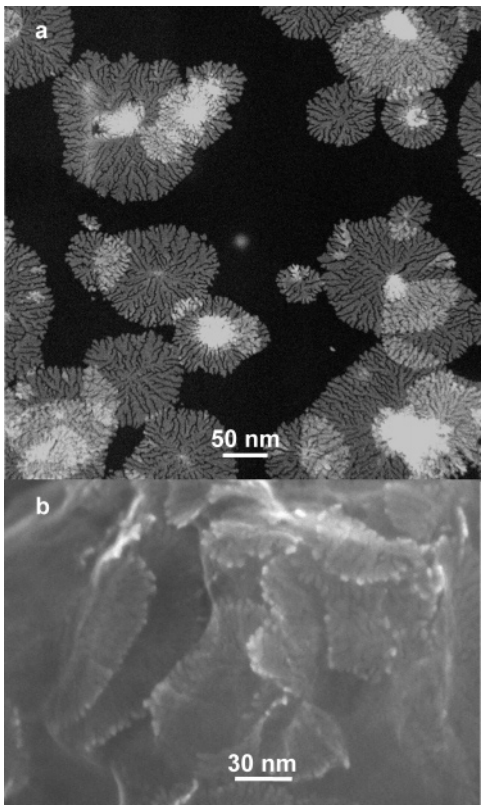


**Figure 4.** (a) HAADF scanning TEM image and (b) SEM image of circular platinum nanosheets grown in the presence of multilamellar DSPC vesicles (400-nm average diameter). Reaction conditions: [Pt] = 10 mM; [AA] = 75 mM; [DSPC] = 0.5 mM.

(average diameter approximately 400 nm) prepared in AA. The large average size and broad size distribution ensure that there are very large vesicles with low curvature available for the formation of large flat circular dendritic sheets such as those shown in Figure 4. In this case, we do not use photocatalytic seeding because we desire only a small number of widely separated growth centers to prevent joining of the growing circular dendrites; thus we rely on the slow spontaneous chemical reduction of Pt complex by AA to produce a small population of growth centers. The material obtained from an optimized reaction using the vesicles as templates was found to be approximately 90% large dendritic platinum nanosheets such as those shown in the HAADF TEM image in Figure 4a. These platinum nanosheets are generally uniform in thickness but show a wide size distribution (30−500 nm). The broad size distribution results from the continuous seed formation during the reaction and consequent wide variation in growth times.

The nanosheets were estimated to be 2-nm thick based on the slightly thicker particle-like peripheral tips of the dendritic arms of the sheets in the HAADF TEM images (Figure 4a). Some sheets show bright spots in the center of the dendrite indicating a thicker layer of platinum. The distance between the arms of the dendrites (arm spacing) in the TEM images is 1−2 nm. The thickness of the sheets was also measured using SEM by packing a large amount of sample onto a silica wafer and finding edges suitable for imaging (Figure 4b). In the SEM images, the edges of stacks of the circular dendritic sheets are found to be approximately 2-nm thick in good agreement with the estimate obtained from the HAADF TEM images. In addition, it is worth pointing out that the arms of the sheets have a preferred crystallographic growth orientation along 111 planes as shown in Figure S1 (Supporting Information).

Figure S2 of Supporting Information illustrates the range of structures that can be obtained when other conditions are used to platinize the multilamellar liposomes. For example, when the concentration of DSPC is low (0.04 mM), the structures tend to grow isotropically to produce globular platinum dendrites, suggesting that the number of vesicles is not sufficient to induce nanosheet growth. Note that the presence of DSPC liposomes does, however, affect the growth process, as in their absence the platinum grows as large chunks of metal.[43] With 0.5 mM or higher concentrations of DSPC, the reactions generate the desired dendritic nanosheets. When other reaction conditions are constant, the concentration of the platinum complex also influences the shape and size of the platinum dendrites (Figure S3, Supporting Information). Dendritic nanosheets are obtained in the presence of the 10 mM platinum complex, whereas the 1 mM platinum complex results in smaller poorly formed sheets and the 0.1 mM platinum complex produces a mixture of nanoparticles and small globular nanodendrites. The low concentration of the Pt complex may change the autocatalytic reaction rate to a range which does not support dendritic sheet formation.

**Synthesis of Foamlike Platinum Nanospheres and Monoliths.** The platinum morphology is significantly altered when unilamellar DSPC liposomes without photocatalyst are prepared in water at neutral pH and solid AA and aqueous Pt salt are added at high concentrations to the reaction system (Figure 5). The nanostructured platinum now appears as nanoscale foam balls composed of joined Pt sheets. The TEM images (e.g., Figure 5a) and HAADF images (e.g., Figure 5b) show that they are made of continuous interwoven dendritic Pt sheets having a thickness of 2 nm. In the HAADF image, the center area of the nanostructure is much lighter than the surrounding region consistent with an overall spherical shape. The SEM images (e.g., Figure 5c) confirm

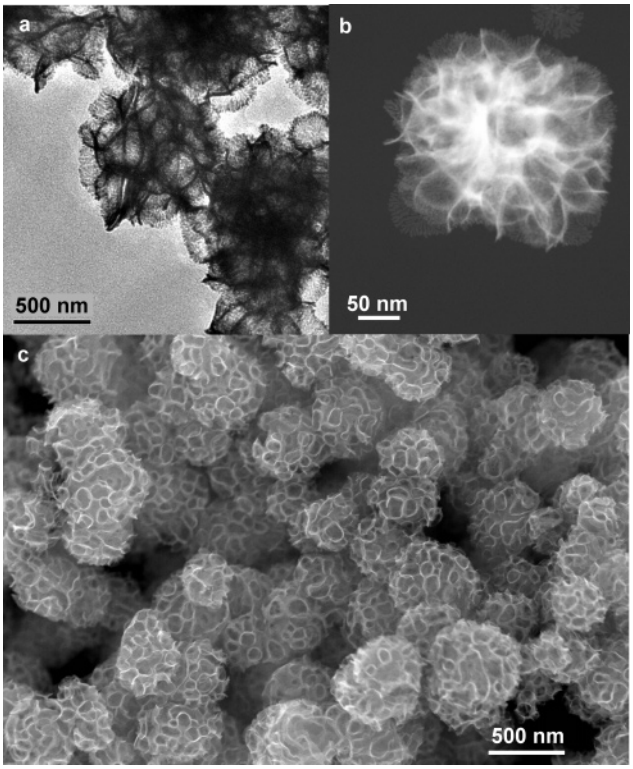


**Figure 5.** (a) TEM image, (b) HAADF scanning TEM image, and (c) SEM image of foamlike platinum nanospheres grown in the presence of 120-nm unilamellar liposomes. Reaction conditions: [Pt] = 10 mM; [AA] = 75 mM; [DSPC] = 0.25 mM; [cholesterol] = 0.25 mM.

the spherical shape and further reveal that these nanospheres possess bowl-like pits on their surface with the typical diameters and shapes of the templating liposomes. The Pt nanospheres prepared using 120-nm liposomes are approximately 350 nm in diameter with a size distribution that is 21% of the average diameter (Supporting Information, Figure S4).

The nanospheres were characterized by XRD and TGA measurements. The powder XRD pattern of the nanospheres (Figure S5, Supporting Information) is similar to that of bulk platinum metal and can be indexed as 111, 200, and 220, respectively. The peaks are broad compared with those of bulk platinum, consistent with the nanoscale feature size of the crystalline dendrites. The bulk sample obtained from the large scale synthesis (Figure S6, Supporting Information) was subject to the DTA/TGA analysis (Figure S7). Below approximately 100 °C, the weight change can be attributed to release of adsorbed water molecules, whereas above 100 °C the weight loss corresponds to the pyrolysis of organic material (presumably surfactant and cholesterol) remaining on the platinum nanofoam. The DTA/TGA measurements indicate that the platinum nanospheres are more than 98% Pt by weight.

The images in Figure 5 strongly indicate that liposomal aggregation plays a significant role in the formation of these remarkable foamlike platinum nanostructures. The surface pits represent liposomes that have not been completely coated with the metal dendritic sheet because the Pt complex available for growth has been exhausted. The structure is not truly a foam because the spherical shapes of the individual liposomes are largely preserved; that is, the liposomes are apparently not distorted to produce the characteristic surface contact angles observed in the cells of true foams. Although some aggregation of the liposomes is induced before metallation as indicated by the flocculates that form immediately after mixing, additional liposomal aggregation may occur during metalation by accretion of liposomes onto the growing dendrite. In any case, the spherical shape likely comes from the initiation of a seed particle followed by isotropic autocatalytic growth along the membranes of the liposomal aggregates until the Pt complex is exhausted (Figure 5c).

To investigate the possibility of controlling the nanostructure of the foamlike Pt spheres, they were synthesized using liposomes of different sizes (average diameters 60−80, 110−120, and 140−170 nm). The TEM and SEM images (not shown) indicate that the average size of the templating liposomes is reflected in the nanoscopic structural features (bowl-like pits) at the surface of the resulting Pt nanospheres. The size of the liposomes did not produce any significant differences in the morphology of the dendrites (arm widths, arm spacings).

**Mechanism of Growth of the Foamlike Platinum Materials.** TEM samples were prepared at specific times during the continuous reaction by washing with water and drying in the air to effectively interrupt the Pt reduction reaction. This procedure gives a snapshot of the nanostructures present at that specific point in time. A study of the time dependence of the growth of foamlike nanospheres using 78-nm liposomes shows the various stages in their development (Figure 6). At 32 min (Figure 6a), dendritic platinum sheets with a small average size and exhibiting little aggregation are observed. By 39 min (Figure 6b), a few separate dendritic sheets are observed, and the foamlike spheres composed of joined dendritic sheets have begun to form. Between 58 and 100 min (Figure 6c), almost all of the metal is present in the form of the foamlike nanospheres with progressively larger average sizes. By 63 min (Figure 6d), the larger and almost mature nanospheres have formed, and by 100 min (Figure 6e), growth has stopped and the mature foam spheres are obtained. High magnification TEM images in the insets of Figure 6 clearly show that the foamlike structures at different stages are composed entirely of interwoven dendritic nanosheets.

Foamlike materials subtly different from those shown in Figure 5 can be obtained when a photocatalyst (2.7 $\mu$M SnOEP) is incorporated into the liposomes and the reaction mixture is irradiated with white light for various time periods to generate growth centers (Figure 7). All of these foamlike structures are composed of convoluted dendritic platinum sheets, which are best seen in the high magnification images in the third column of Figure 7. However, the nanospheres with 10 min of irradiation (Figure 7d1) are clearly smaller than those with no irradiation (Figure 7a1). Longer irradiation times will produce more seed nanoparticles, and the Pt is then distributed over more growth centers to produce smaller nanostructures; the resultant nearly equal growth times will ensure uniform size.[43]

Increasing the number of the growth centers also appears to affect the extent to which the individual nanospheres are

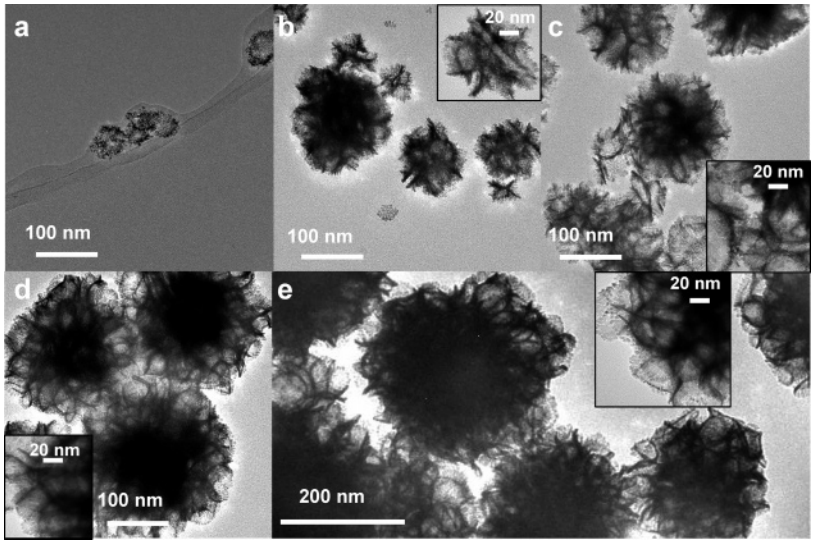


**Figure 6.** TEM images showing the time development of the platinum foamlike nanospheres synthesized in the presence of 78-nm liposomes prepared in water: (a) 32, (b) 39, (c) 58, (d) 63, and (e) 100 min. Inset images are TEM images obtained at higher magnification. Reaction conditions: [Pt] = 10 mM; [AA] = 75 mM; [DSPC] = 0.25 mM; [cholesterol] = 0.25 mM.

interconnected to form a monolithic structure. For example, a comparison of the sample obtained with 10 min of irradiation (Figure 7d2) with that obtained without irradiation (Figure 7a2) indicates much greater intersphere connectivity in the former. This suggests the possibility of fine-tuning the properties of the Pt foamlike materials for specific applications.

To further understand the growth process for the foamlike nanostructures produced by the photocatalytic seeding method, TEM samples were prepared at specific times during the continuous exposure of the reaction to intense incandescent white light (800 nmol·cm$^{-2}$·s$^{-1}$). The TEM sample preparation procedure of washing with water and drying in the air effectively interrupts the reaction and, therefore, gives a snapshot of the nanostructures present at that specific point in time; representative TEM images are shown in Figure 8. At 10 min of irradiation (Figure 8a), small amounts of individual 2−3 nm particles are found on the TEM grid along with some small dendritic sheets with only a few branches. By 13 min (Figure 8b), fewer seed particles are observed and more and larger dendritic sheets are seen, and at 15 min (Figure 8c), almost all the original seed particles have begun to grow into dendrites and most of them already have at least a few branches. After 17 min of irradiation (Figure 8d), the two-dimensional dendrites have grown much larger, they conform to the spherical shape of the liposomes, and they have started to join to neighboring dendritic sheets to form the foamlike structure. By 20 min (Figure 8e), the nanofoam morphology has matured but with small feature size relative to the final product. Finally, at 30 min (Figure 8f) and at longer times, the mature nanofoam is observed with joined networks of the dendritic sheets.

The time-development studies of the two types of foams (Figures 6 and 8) are consistent with a growth mechanism based on spontaneous or photocatalytic nanoparticle seeding and subsequent autocatalytic growth of the seeds into dendrites by reduction of the Pt complex at their surfaces. This mechanism was suggested by us previously to explain the formation of the related globular nanodendrites.[43] The combined results from our studies rule out a rival growth mechanism based on nanoparticle formation followed by aggregation of the nanoparticles to form the dendritic sheets, which was recently suggested for our platinum nanostructures by two independent groups.[52,53]

The mechanism of the templating effect of the unilamellar liposome is poorly understood at the molecular level, but the likely site of Pt growth is suggested by SEM images of platinum foam nanospheres for which the surfactant has not been removed by rinsing with water (Figure 9). (Structures obtained before and after washing away the surfactant layers are also compared in Figure S8.) In the SEM images, the Pt sheets are seen as bright ridges between the surfactant layers. The thickness of the surfactant layers is consistent with a monolayer of the surfactant, suggesting that the dendritic platinum sheet grows within the bilayer of the unilamellar liposome. A caveat is that surfactant could be picked up by the metal surfaces after growth or during sample preparation and drying.

Growth in the organic phase of the bilayer would necessitate access to the catalytic metal surface by the platinum complex and AA. Access to the interior of the membrane is indeed possible because at pH 3 AA is neutral and somewhat hydrophobic, and also a large proportion (42%) of the aged Pt complex is the neutral $Pt(H_2O)_2Cl_2$ species.[50] Thus, it is likely that nutrients can access the growing metal surface of the dendrite inside the bilayer, where AA would be oxidized and the electrons used to reduce the Pt complex producing neutral metal atoms that are deposited onto the growing dendrite. The required neutrality and hydrophobicity of nutrients might partially explain why AA seems to be unique in producing well-formed Pt dendrites; however, specific interactions between AA and the metal surface could also play a role in directing the growth.

In this scenario, another issue is how the growing metal sheet moves from one liposome to another in the foamlike nanospheres and monoliths. If the liposomes in the aggregate fuse together, then the hydrophobic interstitial space in the bilayer of one liposome will be contiguous with that of

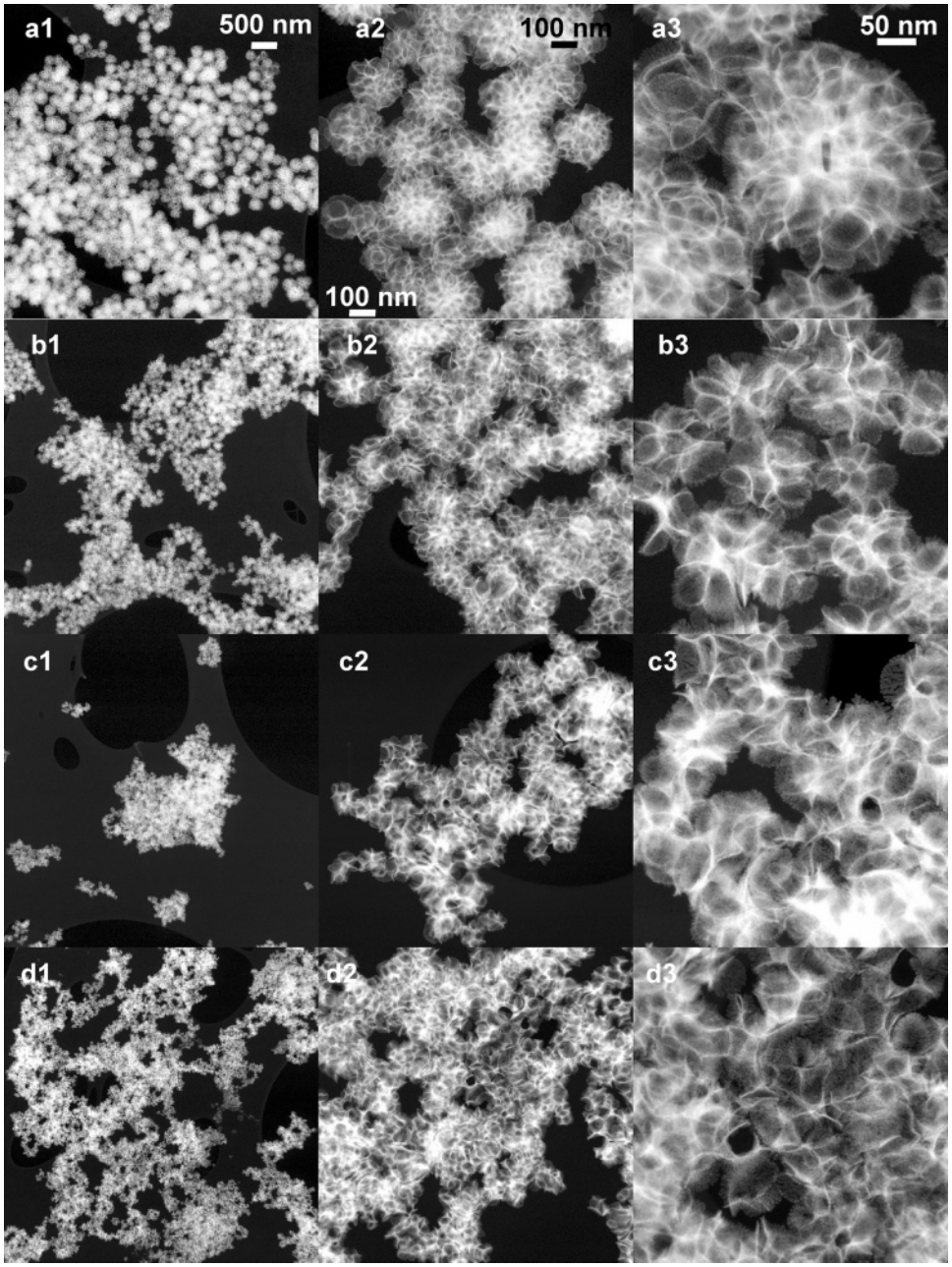


**Figure 7.** HAADF scanning TEM images showing different forms of platinum foamlike nanostructures synthesized in the presence of unilamellar liposomes (average diameter of 110 nm) containing 2.7 $\mu$M SnOEP photocatalyst and prepared in water. Irradiation times with 800 nmol·cm$^{-2}$·s$^{-1}$ incandescent light are 0 (a), 3 (b), 5 (c), and 10 min (d). Images in the same row are the same sample at different magnifications. Reaction conditions: [Pt] = 10 mM; [AA] = 75 mM; [DSPC] = 0.25 mM; [cholesterol] = 0.25 mM.

another, and thus lateral confined growth of the dendritic sheet can continue between the fused liposomes. Alternatively, if the two liposomes are merely in contact with each other, then two layers of lipid separate the hydrophobic regions of the neighboring liposomes, and these layers must be breached for the platinum to continue growing from one liposome to the next. If penetration of the layer is required, this may occur as a result of the noted thickening visible at the centers of many of the dendritic sheets shown in Figures 4a and S2b (Supporting Information). This thickened region may pierce the surfactant layers and possibly induce fusion with an adjacent liposome in the aggregate in which lateral growth continues.

**Surface Areas and Electrocatalytic Activity of the Foamlike Platinum Nanospheres.** The nanofoams shown in Figure 5 are an extraordinary example of a "self-supported" platinum material, which retains its dendritic structure after the removal of the surfactant and drying (see Figure S8) and even upon sonication and re-suspension. They are expected to have good electrical connectivity (compared to the nanoparticles in Pt black, for example) because of their dendritic nature and high degree of crystallinity. They are also highly porous on different length scales. These features are desirable in catalytic and electrocatalytic applications such as fuel cells. It is, therefore, important to characterize the platinum foamlike materials to determine their potential as catalysts. Accordingly, we have measured their surface areas using nitrogen adsorption experiments, their active surface areas using CO-stripping methods, and their electrocatalytic activity in the ORR.

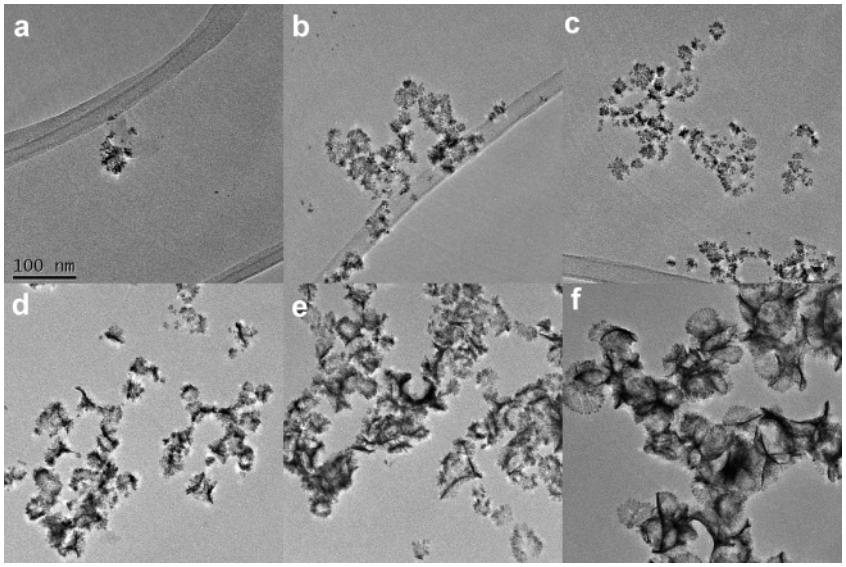


**Figure 8.** TEM images showing the time development of the platinum foamlike nanospheres synthesized using 78-nm liposomes containing 2.2 $\mu$M SnOEP prepared in water: (a) 10, (b) 13, (c) 15, (d) 17, (e) 20, and (f) 30 min. Reaction conditions: [Pt] = 10 mM; [AA] = 75 mM; [DSPC] = 0.25 mM; [cholesterol] = 0.25 mM.

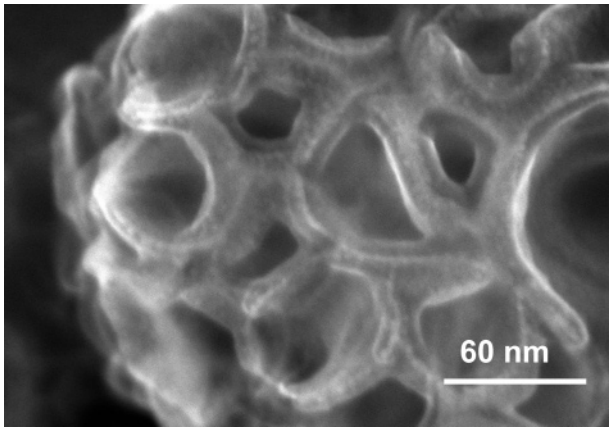


**Figure 9.** SEM image showing a platinum foam nanosphere synthesized in the presence of 78-nm liposomes prepared in water. Reaction conditions: [Pt] = 10 mM; [AA] = 75 mM; [DSPC] = 0.25 mM; [cholesterol] = 0.25 mM.

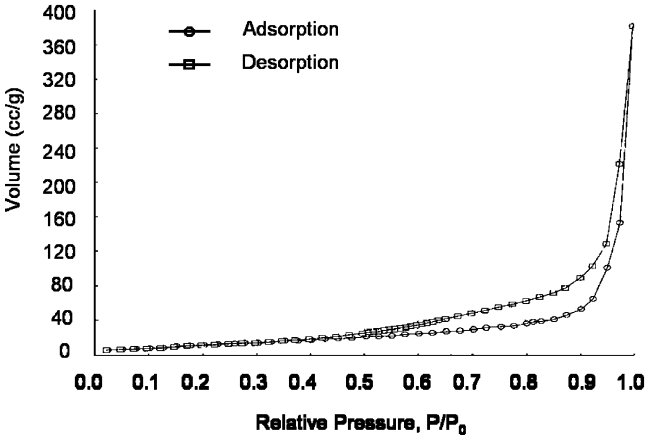


**Figure 10.** Typical isotherm obtained from the nanospheres nanofoams after surface cleaning.

Figure 10 shows a typical nitrogen adsorption/desorption isotherm for the platinum nanospheres from which the average surface was determined. The foam nanospheres made with 78-nm and 140-nm liposomes have similar surface areas of 26.9 $\pm$ 0.5 $m^2/g$ based on multiple repetitions of the $N_2$ adsorption measurements. This surface area may be lowered somewhat by the loss of the smallest platinum nanospheres in the washing procedure used to remove surfactant. Although all of the surfactant may not have been removed by our procedure, ozone plasma treatment of the foam nanospheres for 1 h, which should have decomposed any surfactant remaining on the platinum surface, gave an identical BET surface area. The average surface area obtained is comparable to the surface areas of the commercially available platinum black used in fuel cell applications (ETEK, Sigma-Aldrich). These Pt black materials are typically composed of 5−6 nm particles. The isotherm loop evident in Figure 10 also confirms that the material is porous, presumably due to the random packing of the nanospheres, spaces between the arms of the dendrites, and the open spaces produced by the templating liposomes.

Thin films of Pt nanospheres made with 140-nm and 78-nm liposomes (abbreviated as Pt 140 nm and Pt 78 nm in the figures) as well as Pt black (ETEK) were prepared, and cyclic voltammetry experiments were performed in $N_2$ sparged 0.5 M $H_2SO_4$. Cyclic voltammograms (CVs) were run at 50 mV/s from just positive of the hydrogen evolution potential (0 $mV_{RHE}$) to about 1500 $mV_{RHE}$; this potential window is useful for evaluating electroactive Pt materials. Typical CVs acquired for the Pt nanospheres are shown in Figure 11. Features associated with hydrogen adsorption and desorption events (cathodic and anodic peaks at potentials of approximately 100−200 $mV_{RHE}$) and the reduction of surface oxide (at about 750$mV_{RHE}$) are seen in the CVs for each sample. These features are characteristic of polycrystalline Pt.[54] Multiple peaks (rather than a single broad peak) for hydrogen adsorption and desorption are indicative of multiple exposed crystallographic planes, consistent with the XRD data given in Figure S5 (Supporting Information). Thus, the data in Figure 11 show that the nanostructured Pt foams

(54) Paulus, U. A.; Schmidt, T. J.; Gasteiger, H. A.; Behm, R. J. *J. Electroanal. Chem.* **2001**, *495*, 134−145.

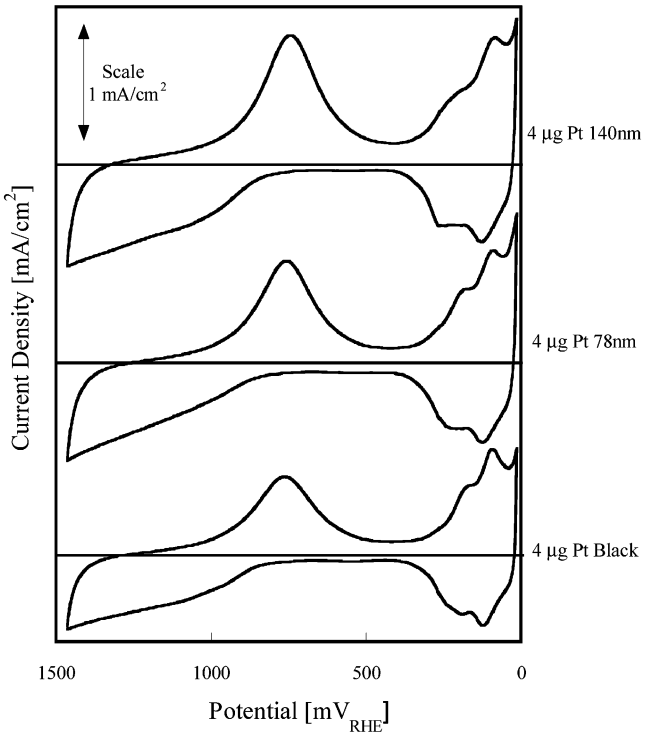


**Figure 11.** CVs of Pt nanospheres with 140-nm and 78-nm liposomes compared to that of Pt black (ETEK). CVs were run in a $N_2$ sparged 0.5 M $H_2SO_4$ electrolyte at 50 mV/s. The loading is 4 $\mu$g of Pt for each sample, and current density is based on the geometric surface area of the GCEs used (0.0707 cm$^2$). Note the hydrogen adsorption/desorption features at ca. 100−200 mV$_{RHE}$.

behave in qualitatively the same way as polycrystalline platinum.

In addition, the Pt foam nanospheres possess an electroactive surface area that is similar to that of Pt black, as evidenced by the current associated with the hydrogen adsorption and desorption events. (Because the Pt loading of 4 $\mu g_{Pt}$ for each sample tested is the same, the current in this region correlates directly to surface area differences between the samples.) The electroactive surface area can be quantified by integrating the current associated with these events, although in the present work we utilized CO-stripping experiments to quantify the electroactive surface areas.

CO-stripping voltammograms of the nanospheres and the Pt black samples as well as the methodology for calculating the electroactive surface area are presented in the Supporting Information text and in Figures S9 and S10. The measured surface areas are 15.5 ± 1.4, 16.8 ± 2.9, and 18.1 ± 0.9 $m^2/g_{Pt}$ for Pt black (ETEK), Pt 140 nm, Pt 78 nm, respectively. Statistically, the 78-nm liposome material has a larger surface area than the ETEK Pt black, meaning more sites are available for electrochemistry for the same amount of Pt metal. Given the variance associated with the reported values,[55−57] however, the most conservative conclusion is that the nanospheres have at least as much electroactive surface area per unit mass as the ETEK material.

The ORR was also probed via rotating disk electrode (RDE) experiments to compare ORR activities of these materials and to see which of the following two reactions the Pt foams catalyze:

$$O_2 + 2H^+ + 2e^- \rightarrow H_2O_2$$

$$O_2 + 4H^+ + 4e^- \rightarrow 2H_2O$$

The $4e^-$ reduction of oxygen to $H_2O$ is preferred for fuel cells because reduction to $H_2O_2$ has a lower potential and causes cell degradation. Details of the ORR experiments and data analysis are given in the Supporting Information text and in Figures S11−S13. Qualitatively, the shape of the ORR curve is very similar for each sample, indicating comparable kinetics and confirming that Pt foam nanospheres have electrocatalytic behavior similar to the Pt black material. It was found that the Pt foams, as well as Pt black, generally catalyze the $4e^-$ ORR with only the Pt 78 nm sample having a value of $n$ that is statistically less than 4.

In summary, the Pt foams have electroactive surface areas and electrocatalytic activities comparable to those of Pt black, but rather than consisting of a distribution of nanoparticles that may be unconnected, these dendritic foamlike materials are nanostructured and behave somewhat like polycrystalline platinum. For example, the Pt nanospheres and monoliths should be highly conductive over hundreds of nanometers, that is, the diameters of the nanospheres. More detailed electrochemical evaluations of the Pt foam materials are ongoing for use as fuel cell electrocatalysts and in other applications.

## Conclusions

A series of dendritic platinum nanostructures, including small uniform-sized nanosheets, large circular nanosheets, discrete foamlike nanospheres, and extended and networked foamlike materials were synthesized with controlled feature sizes using liposomal templates prepared in water or AA solutions. All of these materials are composed of flat or convoluted dendritic sheets of platinum metal that are nominally 2-nm thick with 3−4-nm wide arms and 1−2-nm arm spacings. Photocatalytic seeding using a tin porphyrin photocatalyst and visible light provides a facile and versatile means of producing the desired number of dendritic growth centers at the desired time in the reaction. This method of producing growth centers provides a straightforward means of controlling the product size, size distribution, and other structural features.

The foamlike nanospheres and monoliths are self-supported platinum materials with multiple levels of porosity, one determined by the size of the liposomes upon which the foamlike materials are fashioned and another associated with the 1−2 nm spacing of the dendritic arms. Time-evolution studies of the platinum nanofoams are consistent with a mechanism in which photocatalytically or spontaneously generated seed nanoparticles grow by catalytic oxidation of AA and reduction of the platinum complex with the metal being deposited at the surface of the growing dendrite. The data presented in this work and in our previous studies[43]

(55) Itoe, R. N.; Wesson, G. D.; Kalu, E. E. *J. Electrochem. Soc.* **2000**, *147*, 2445−2450.
(56) Mello, R. M.; Ticianelli, E. A. *Electrochim. Acta* **1997**, *42*, 1031−1039.
(57) Perez, J.; Gonzalez, E. R.; Ticianelli, E. A. *Electrochim. Acta* **1998**, *44*, 1329−1339.

support this mechanism rather than one based on nanoparticle generation and subsequent particle aggregation.[52,53] New SEM images suggest that the nanosheets grow between the liposomal bilayers. In addition, the present results raise the possibility of attaching porphyrin labels to membrane-bound biological molecules such as proteins, lipids, and drugs and subsequently photocatalytically growing "nano-tags" (nanoparticles and small dendrites) at the location of the bound molecule. The nanotags can then be used to image the location of these porphyrin-labeled components at nanometer resolution by TEM techniques.

The platinum foams are very attractive from the standpoint of electrocatalytic reactions such as in PEM fuel cell applications. Not only do they have high BET and electroactive surface areas comparable to high surface area commercial platinum black, but the extended open dendritic structures may provide better current conductivity than the nanoparticles in Pt black. For example, the foamlike materials may avoid the need for conducting supports such as carbon black thereby reducing the thickness of the catalyst layer of the membrane electrode assembly (MEA) of PEM fuel cells. The potential advantage of thin catalyst layers in PEM fuel cells has been noted by Debe,[58] who used platinum deposited on organic whiskers to build a MEA. The thin catalyst layer provides a higher heat and water generation rate per unit volume, more efficient usage of the catalyst at all current densities, and a shorter electrode ionic resistive path. The latter results from the fact that the protons have a shorter distance to percolate between the PEM and the reactive catalyst surface sites compared to the conventional thick catalyst layer produced using 3−5 nm platinum particles supported on carbon.[58] The porosity of the platinum nanofoam materials should also facilitate the mass transport in electrocatalytic applications, which may lead to increased current densities. Finally, their dendritic morphology may lead to increased stability of the platinum foamlike materials in catalytic applications.

**Acknowledgment.** This work was partially supported by the Division of Materials Sciences and Engineering, Office of Basic Energy Sciences, U.S. Department of Energy, and by the Division of Chemical Sciences, Geosciences and Biosciences, Office of Basic Energy Sciences, U.S. Department of Energy (DE-FG02-02ER15369). Sandia is a multiprogram laboratory operated by Sandia Corporation, a Lockheed Martin Company, for the U.S. Department of Energy's National Nuclear Security Administration under Contract No. DEAC04-94AL85000.

**Supporting Information Available:** Additional TEM and SEM images of the platinum nanosheets and foamlike nanostructure; size distribution of the Pt foam nanospheres; a typical XRD pattern of the platinum nanospheres; a photograph of a bulk sample of the platinum foam nanospheres; DTA/TGA diagram obtained for the platinum nanospheres; representative CO-stripping and ORR voltammograms; and details of the calculations of electroactive surface areas and analysis of the ORR data (Levich and Tafel plots; PDF). This material is available free of charge via the Internet at http://pubs.acs.org.

CM060384D

(58) Debe, M. K. *Handbook of Fuel Cells Fundamentals, Technology and Applications*; John Wiley & Sons: New York, 2003; pp 576−588.